ANTI-REFLECTION-COATING THICKNESS MEASUREMENTS ON TEXTURED SILICON SURFACES: EVALUATION AND ACCURACY OF DIFFERENT MEASUREMENT TECHNIQUES

Alexander Krieg, Johannes Greulich, Marcel Tondorf, Stefan Rein
Fraunhofer Institute for Solar Energy Systems ISE, Heidenhofstr. 2, D-79110 Freiburg, Germany

ABSTRACT: The accuracy and reliability of different techniques for inline quality control of antireflection coatings (ARC) on industrial relevant surfaces are analyzed and rules to improve the accuracy of the systems are derived. For this, four systems are compared with respect to the setup and the way of ARC thickness calculation. Raw data and measured thicknesses are evaluated with respect to a reference system, to identify for each surface texture the system which is suited best and to identify the physical reasons for deviations. Angle-dependent simulations and measurements of the spectral reflectance on monocrystalline wafers with a pyramidally-etched surface reveal that different angle corrections for mc-Si and Cz-Si are required. Besides evaluating the spectral position of the reflectance minimum, a least-squares fit of the spectral reflectance of partially textured Cz-Si is presented and evaluated.

Keywords: antireflection-coating, surface texture, quality control, inline measurement

1 INTRODUCTION

Research on silicon solar cells aims at high efficiencies at low cost. Efficiency is directly related to short circuit current, which in turn strongly depends on surface texture and the thickness of the anti-reflection coating (ARC). In the present work, a variety of systems for controlling the ARC thickness is evaluated thoroughly including spectroscopy (with integrating sphere and direct illumination) and camera-based methods. The system geometries and the measurement principles of the systems are reviewed. Since the surfaces of solar cells are generally not flat, the wavelength of the reflectance minimum shifts due to the rough wafer surface in comparison to a planar surface. So far, when determining the ARC thickness from reflectance data only the wavelength of the reflectance minimum is evaluated without taking into account any impact of the surface texture. In the present work, the accuracy of this simplified data analysis is evaluated. Moreover, a different approach based on a modelling of the spectral hemispherical reflectance is presented and applied to coated, (partially) textured mono-crystalline Cz-Si samples.

2 EXPERIMENTAL

To evaluate the accuracy of different techniques for ARC thickness (d_{ARC}) measurements with respect to an impact of the surface morphology, a set of test samples has been prepared that consists of mono- and multi-crystalline silicon wafers with different surface textures (alkaline etched with varied pyramid size and coverage, acidic etched with different texture strength) and different coating thicknesses. The wafers were measured at almost identical positions with the different instruments. In order to compare the data correctly, two reference techniques have been established. As a reference for the layer thickness measurement a highly accurate spectrophotometer was used, while the reference values for the refractive index have been determined with a laser-ellipsometer.

2.1 Test samples

2.1.1 Alkaline textured wafers

The set of alkaline-textured mono-crystalline test wafers consists of 54 Czochralski silicon (Cz-Si) wafers, which were all damage-etched in the first process step. Subsequently, the surfaces were textured on both sides in an alkaline etching process with random pyramids, the pyramid size and the degree of coverage being varied by changing the chemical concentration and the process time. Among the test sample the total area covered with pyramids varied between 82%, 98% and 100%. The degree of coverage was determined from confocal micrographs with an image processing algorithm [1], which detects the shiny non-textured regions, as shown in Figure 1. Finally, the wafers were coated with a PECVD antireflection-coating in a thickness range from 60 to 100 nm.

Table I: Pyramid coverage and related reflectance data for the three Cz-Si wafer groups with different alkaline surface textures.

Texture	complete	some defects	many defects
Degree of pyramid coverage	100%	98%	82%
Reflectance @ 600 nm after texturization	11%	12%	14%

2.1.2 Acidic textured wafers

Within the set of acidic-textured multicrystalline wafers, the acidic texture (HF/HNO_3) was varied three-fold in an inline processing tool. The variation of the texture was achieved by changing the process time among the three process groups with 10 wafers/group. To characterize the acidic texture, confocal micrographs were taken, as shown in Figure 2, and the surface

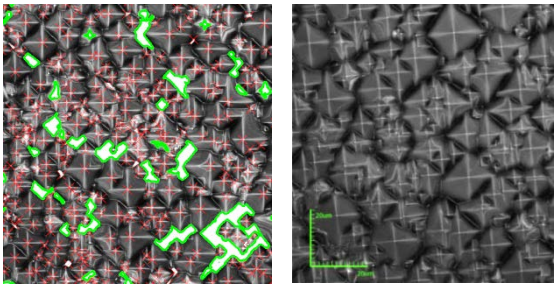

Figure 1: Laser intensity images of alkaline textured wafers with a pyramid coverage of 82% (left) and 100% (right) taken by a confocal microscope. An image processing algorithm detects the shiny non-textured regions (green border).

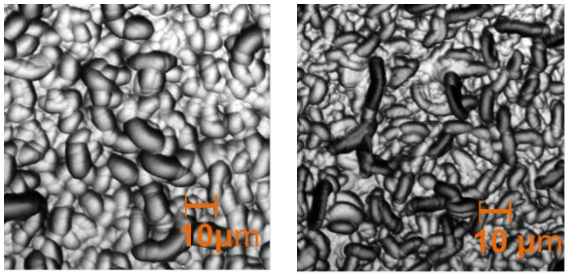

Figure 2: Laser intensity images of acidic etched wafers with a soft (left) and a strong (right) texture taken with a confocal microscope.

enlargement was determined, which is calculated as the ratio of the textured surface to the plane surface (see e.g. [2]). The reflectance was measured by a spectrophotometer directly after the process (Table II).

Table II: Surface enlargement and related reflectance data for the three mc-Si wafer groups with different acidic surface textures.

Texture	soft	standard	strong
Surface enlargement	1.3	1.6	1.7
Reflectance @ 600 nm after texturization	32%	27%	25%

2.2 Measurement instruments

In the present work, the following four systems for controlling the ARC thickness are evaluated.

2.2.1 Reference measurement instruments

With a laser-ellipsometer the refractive index of the SiNx layer of 2.01 at $\lambda = 633$ nm was determined on a planar reference sample which was processed concurrently with the test samples. Thus, all layer thickness data presented hereafter are based on a refractive index of $n_1 = 2.01$ in order to ensure the comparability of measurements. The textured samples were tilted during the measurement so that the pyramid's facets are aligned perpendicular to the plane of incidence and detection of the ellipsometer. The planar and acidic textured samples were not tilted.

For reference measurements of the spectrally resolved reflectance curves, a Cary 5000 UV-Vis-spectrophotometer was used with a double out-of-plane Littrow monochromator and wavelength accuracy of ± 0.1 nm in the considered range. Among the investigated instruments it is the only instrument that can determine the wavelength in 1 nm steps and provides very reliable reflectance values over the entire spectral range from 175 to 3300 nm. The system has an integrating sphere and a direct monochromatic illumination. The wafer is arranged in an angle of 7° with respect to the primary beam during the measurement (Figure 3). The primary beam is diffusely reflected at the wafer surface and reaches the detector via the integrating sphere.

To examine the intensity of the primary beam, a second monitor beam is sent directly to the reflection standard 1. The light is scattered at the standard (and the integrating sphere) to be finally registered in the detector. The two beams are sent alternately by means of a chopper into the integrating sphere. The system is calibrated with a diffuse white standard.

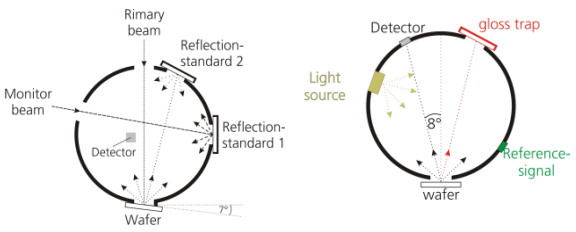

Figure 3: Scheme of the integrating spheres of the highly accurate spectrophotometer (left) and the fast inline suitable spectrophotometer (right).

2.2.2 Fast inline-suitable spectrophotometer

The fast inline spectrometer allows a measurement of a reflectance spectrum of a wafer in the wavelength range from 310 to 1100 nm within one second, thus the system is suitable for inline measurements. In contrast to the reference spectrometer, the wafer is diffusely illuminated by a halogen lamp that is integrated into an integrating sphere and ensures a broad-band illumination. The respective wavelength is measured by means of a multichannel spectrometer with a measuring step width of 3 nm. The detector is inclined by 8° perpendicular to the wafer. For calibration, a diffuse grey standard with a reflectance of 10% was used.

2.2.3 Multichannel CCD-spectrometer

The spectral measurement is realized in this case with a CCD-matrix camera which spatially resolved reflectance measurements in a wavelength range from 400 to 800 nm. To obtain a spatially resolved measurement, the sample must be measured on-the-fly. The multichannel spectrometer measures 100 single spectra transverse to the transport direction of the wafer and records 100 lines of spectra in transport direction along the moving wafer. With this setup 10000 single spectra on the wafer are available in a measuring time of 6 seconds. In an inline application, spectra at 100x20 points can be measured within a cycle time of 1 second. For each spectrum, the minimum of reflection and the thickness is calculated with a predefined refractive index of 2.01, resulting in a ARC thickness topography with 100x100 points. For the comparison of the different systems, the thickness in the middle of the wafer is used. In the setup, the wafer is illuminated directly by a line of LEDs, which is approximately inclined by 8° to the wafer normal. The reflected light is detected at an angle of 8° to the wafer normal. The system is not calibrated to absolute reflection values, as only the position of the minimum is required for the determination of the layer thickness d_{ARC}.

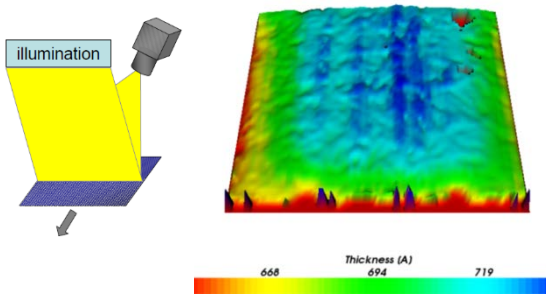

Figure 4: Scheme of the multichannel spectrometer system (left) and a 3D plot of the ARC thickness measured by means of spectral reflectance over the whole area of a 156x156 m^2 Cz-Si wafer (right).

2.2.3 Camera-based inline inspection system

The camera-based inline inspection system Figure 5, which is integrated in a cell tester, consists of a line camera with a resolution of 1365 RGB-pixel and a pixel size of 168 x 168 µm². The wafers are illuminated with a cold light neon tube, whose spectrum simulates daylight. The wafers are in motion and fixed by vacuum at the conveyor belt to ensure a flat surface [3]. For the calibration of the camera-based system, the reference thicknesses of a set of calibration wafers are assigned to RGB colors.

Figure 5: Camera-based inspection system.

2.3 Methods for ARC-thickness determination from reflectance data

For the whole set of test samples, the ARC thicknesses are determined with the different tools using different methods of data analysis, which should be briefly summarized. In case of the spectrometer systems, the thickness $d_\perp$ is calculated from the wavelength λ_{min} at the minimum of the reflectance curve according to:

$$d_\perp = \frac{\lambda_{min}}{4n_1} \quad (1)$$

with n_1 being the refractive index of the dielectric layer. If the detection occurs not perpendicular to the surface of the sample, the incident angle θ has to be considered and the thickness has been calculated according to:

$$d_\theta = \frac{\lambda_{min}}{4n_1} \cdot \sqrt{1 + \frac{n_0^2}{n_1^2} \sin^2(90° - \theta)} \quad (2)$$

where n_0 is the refractive index of the surrounding medium, which is air in the present case ($n_0 = 1$).

The thickness calculation of the camera-based system test wafers is based on the assignment of extracted colors of the test wafer to calibrated colors by determining the shortest interval in relation to the calibrated color in the 3D-RGB-color space.

3 RESULTS

3.1 Accuracy and reliability of different techniques for inline-quality control of AR coatings

The ARC thickness has been measured on the whole set of Cz-Si and mc-Si test wafers using the different techniques, the results being compared with results from the reference system. Figure 6 shows the results for samples with all types of surface morphologies for an exemplary layer thickness of 73 nm.

The deviations of the fast inline-suitable spectrophotometer to the reference measurements on Cz-Si and mc-Si wafers are smaller than 1.5 nm for the whole variety of surface morphologies which is sufficient for a reliable process control (Figure 6).

The differences of the thickness measured with the multi-channel CCD-spectrometer for all variants of the acidic etched mc-Si wafers are also in sufficient range of +2 nm. No impact of the surface morphology can be observed. On Cz-Si wafers the CCD-spectrometer shows a discernible impact to the degree of texture (Figure 6). This may be explained by the following observation. For a given ARC thickness, the minimum of the reflectance curve of a planar wafer is shifted to an approximately 15 nm larger wavelength than that of an alkaline textured wafer due to the absence and presence of multiple reflections (see section 3.2). In the CCD-spectrometer, most rays reflected by the textured part of the surface cannot reach the detector due to the directed illumination and directed detection, whereas in the reference setup with integrating Ulbricht sphere, all rays reflected by the textured part of the surface do reach the detector. As rays coming from the planar parts of the surface are primarily reflected directed, their detection rate is similar in the CCD- and the offline-spectrometer. Therefore, in the CCD-spectrometer, the planar parts result in a larger detected signal than the textured parts compared to the reference setup with an integrating Ulbricht sphere. The wavelength of the reflectance minimum in the CCD-spectrometer is dominated by the planar parts resulting in an over-estimation of the film thickness for partially textured Cz Si compared to the setup with Ulbricht sphere.

The thickness measured with the camera-based inline inspection system differs about 1 nm in case of fully textured Cz-Si wafers (Figure 6). On the partially untextured wafers, the differences rise up to 2 nm because with the flat areas the brightness and thus the layer thickness rise. However, a difference of 2 nm reached with this system is sufficient for a reliable process control. Mc-Si wafers have not been investigated.

3.2 Angle-dependent measurements

When inclining a plane sample with an ARC thickness $d_\perp$, a shift of the reflection minimum to shorter wavelengths is measured. The theoretical shift of the reflection minimum in terms of wavelength depends on the angle between the direction of detection and the normal of the wafer surface according to equation (2) and is shown in Figure 7.

In angle-dependent reflection measurements on monocrystalline wafers with a pyramidally-etched surface, the position of the reflection minimum differs greatly from the values for flat surfaces (Figure 7, red symbols). This is due to the existing preferential directions of the orientation of the pyramids and thus due to the related multiple reflections on the surface. As the pyramid side faces are inclined at 54.75° to the surface, incident light rays are reflected again to the 54.75° inclined pyramid flanks of neighbor pyramids before they are detected by the measuring device. The number of reflections and the shift of the reflectance minimum were calculated with the ray tracer OPAL 2 [4] and are shown as a function of the angle of incidence in Figure 7 for

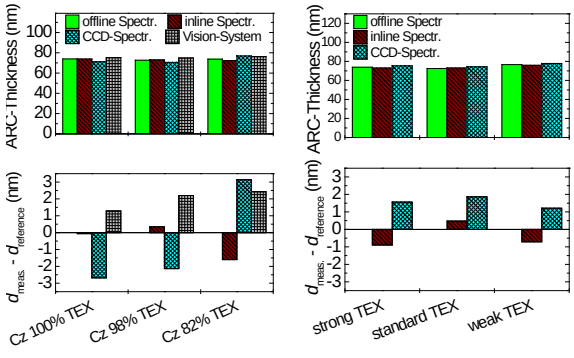

Figure 6: (Top) ARC-thickness measured with the evaluated systems and (bottom) the deviations to the reference spectrometer for Cz-Si (left) and mc-Si (right).

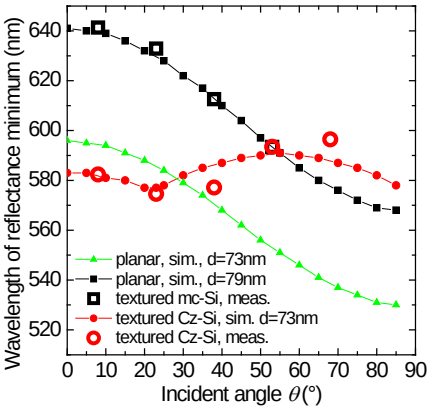

Figure 7: (Top) Shift of the reflection minimum as a function of the angle of incidence simulated by means of OPAL 2 ray tracer and measured on Cz-Si and mc-Si wafers with different surface morphologies.

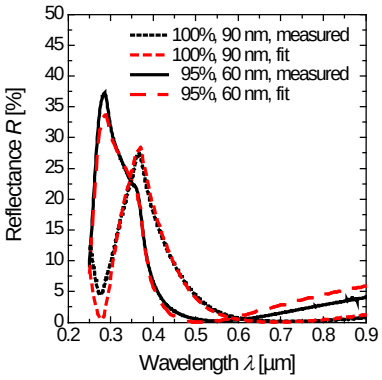

Figure 8*:* The reflectance of a sample with a = 100% and d_{ARC} = 90 nm and of a second sample with a = 95% and d_{ARC} = 60 nm are shown. The measured spectral reflectances (black lines) match roughly with the fitted curves (red lines).

different surface morphologies. For comparison the reflectance minima have also been determined from angle-dependent reflectance measurements on acidic-textured mc-Si and alkaline-textured Cz-Si wafers, which are also shown in Figure 7.

As can be seen in Figure 7 from the simulations for an alkaline textured surface (red symbols), the position shift of the reflectance minimum (compared to the vertical measurement at $\theta = 0°$ on textured Si) ranges between -6 nm and +8 nm , respectively, when measuring the wafer at an angle of $\theta = 23°$ and $\theta = 55°$, respectively. As can be seen, the theoretical expectations are well reflected by the measured data (open symbols). The error in determining the ARC-thickness resulting from the angle dependent shift of the minimum position is approximately 1 nm. This means that an alkaline textured surface diffuses light sufficiently, such that a shift of the reflectance minimum due to variations in the angle of incidence needs not necessarily to be taken into account.

Another aspect is the comparison of the wavelength of the reflectance minimum of textured and planar surfaces. For the case shown in Figure 7, the positions of the minima differ by 596 nm - 583 nm = 13 nm at $\theta \approx 0°$. According to equation (1), this induces an apparent difference in the determined film thickness of 12 nm/4/2.03 ≈ 1.5 nm, even though the true thickness is the same for both surfaces. Further simulations show that using equation (1), the surface texture and the assumption of a constant refractive index n = 2.03 induce ARC thickness errors of less than ± 2 nm for ARC thicknesses ranging from 60 nm to 80 nm.

In contrast to that, mc-Si wafers with acidic-textured surfaces reflect the light under different detection angles similar to wafers with a flat surface. When determining the layer thickness from measurements not made perpendicular to the sample surface, the angular influence on the reflectance must be considered according to the equation (3) in order to avoid systematic errors.

3.3 Fitting the ARC thickness with the transfer-matrix formalism

So far, the wavelength of the reflectance minimum has been evaluated in order to determine the ARC thickness. In this section, a different approach is presented and applied to the coated, (partially) textured Cz-Si samples. This approach is based on a model of the spectral hemispherical reflectance. The contributions of the planar and the textured parts of the surface are assumed as being independent from each other. Based on Fresnel's equations, the reflectance of the planar part $R_{\mathrm{plan}}(\lambda)$ is calculated with the transfer-matrix formalism [5] as mean of the transverse electric and transverse magnetic waves, since the illumination in the spectrophotometer is unpolarized. The reflectance of the textured part $R_{\mathrm{text}}(\lambda)$ is calculated in a similar way using the transfer-matrix formalism. The alkaline texture results in random pyramids, which is modeled here assuming the angles and respective probabilities as compiled by Baker-Finch and McIntosh for normally incident light [6]. The total spectral hemispherical reflectance R_{tot} of a partially alkaline textured and partially flat silicon surface

$$R_{\mathrm{tot}}(\lambda) = (1 - a) \cdot R_{\mathrm{plan}}(\lambda) + a \cdot R_{\mathrm{text}}(\lambda) \qquad (3)$$

is calculated as area-weighted sum of the reflectance of the textured areas R_{text} and of the planar areas R_{plan}, where a denotes the area ratio of the textured part. With a Levenberg-Marquardt algorithm, the area ratio of the textured part a and the ARC thickness d_{ARC} are optimized so that the sum of squares of the deviations between the simulated and the measured reflectance becomes minimal (least-squares fit). For the simulation and the curve fit of $R_{\mathrm{tot}}(\lambda)$, all involved refractive indices have to be known including their dispersion. That of silicon is taken from literature [7] and that of the anti-reflection coating is measured with spectral ellipsometry on planar reference samples. In order to avoid an impact from the backside of the samples due to the so-called escape light, the reflectance is evaluated only up to a wavelength of 0.9 µm.

The spectral reflectance of two samples with differing d_{ARC} and differing a is exemplarily shown in Figure 8. An apparently good match of measured and fitted curves can be observed. However, for wavelengths below approximately 0.6 µm, the fitted curves show a smaller reflectance than the measured ones, whereas this trend is inverted above 0.6 µm. The minima of the fitted reflectance spectra occur at smaller wavelengths than in the measured reflectance spectra (see Figure 8). These observed deviations are reflected by the mean reduced chi-squared χ^2_{red} = 2.0 ± 1.2.

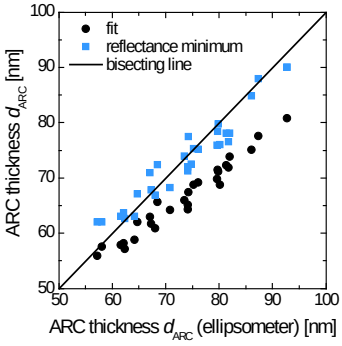

Figure 9: Comparison of different techniques to determine the ARC thickness on alkaline textured Cz-Si samples. The simple evaluation of the reflectance minimum (blue symbols) yields a rather good correlation to the ARC thickness measured with a laser ellipsometer. The fit procedure (black symbols) underestimates substantially the ARC thickness.

Figure 9 shows the ARC thickness on alkaline textured mono-crystalline samples determined from the reflectance minimum (blue symbols) and a fit to the spectral reflectance (black symbols), respectively, in comparison to ellipsometric measurements which have been performed under an angle 35° the refractive index being fixed to the value of $n = 2.01$ which has been determined on a planar reference sample. As can be seen in Figure 9, the curve fit systematically underestimates the ARC thickness compared to the measurement with the laser ellipsometer. The mean absolute error (MAE) over the whole ARC thickness range is 7.0 nm and increases systematically with increasing layer thickness from less than 2 nm to 12 nm. The deviating positions of the minima in the measured and fitted reflectance curves reflect this deviation in Figure 8. In contrast to the fit, the simple approach of evaluating the wavelength of the reflectance minimum yields a better agreement with a MAE = 2.3 nm over the whole ARC thickness range.The underestimation of the ARC thickness in the curve fit approach can be explained with the hypothesis that the optical model used in the fit algorithm underestimates the true reflectance of the samples in the visible and the IR for $\lambda > 0.4$ µm. The algorithm automatically reduces the ARC thickness and the pyramidal coverage below their true values to fit the measured reflectance in the UV. A further development of the model should include the true angle of incidence of 8° instead of assuming normal incidence and the coupling of planar and textured parts in order to increase the algorithm's accuracy.

5 CONCLUSION & OUTLOOK

Different measurement systems and methods for the ARC-thickness determination have been evaluated in terms of their accuracy on industrially relevant surface morphologies.

Using a system with integrating sphere, the thickness determination from the spectral reflectance curve with the minimum method provides precise results on acidic-textured mc-Si wafers and alkaline-textured Cz-Si wafers. On acidic textured mc-Si wafers, precise values can even be extracted from the minimum of the direct spectral reflectance curve measured by means of a multichannel CCD-spectrometer, which has the further advantage of spatial resolution. Using the CCD-spectrometer on alkaline Cz-Si wafers, the ARC thickness is underestimated on fully textured wafers and overestimated on partly untextured wafers. The camera-based system works well, even with Cz texture variations. The deviations to the reference system are always smaller than 3 nm.

The angle-dependent simulations and measurements of the spectral reflectance on monocrystalline wafers with a pyramidally-etched surface revealed that different angle corrections are required for alkaline-textured Cz-Si compared to acidic-textured mc-Si surfaces. For typical detection angles in integrating spheres of 7° and 8°, no angle correction is necessary because the deviations in thickness are below 2 nm.

For the analyzed film thicknesses between 55 nm and 95 nm on alkaline textured Cz-Si surfaces, the SiNx thickness obtained with a least-squares fit to the spectral reflectance is systematically smaller than that obtained with ellipsometry. The reached mean absolute error of 7.0 nm is approximately by a factor 3 larger than that of a simpler evaluation of the wavelength at the reflectance minimum. Therefore, the discussed extended approach cannot be recommended in the present stage for determining the film thickness on partially textured Cz-Si.

5 ACKNOWLEDGMENTS

The authors would like to thank the whole PV-TEC staff for wafer processing. This work has been the German Ministry for the Environment, Nature Conservation and Nuclear Safety (BMU) under the frame of the project QUASSIM (0325132A).

6 REFERENCES

[1] K. Birmann, M. Demant, and S. Rein, "Optical characterization of random pyramid texturization," in *Proceedings of the 26th European Photovoltaic Solar Energy Conference and Exhibition*, Hamburg, Germany, 2011, pp. 1454-8.

[2] J. Nievendick, M. Zimmer, F. Souren, J. Haunschild, M. Demant, and A. Krieg, "Appearance of surface defects created by acidic texturization and their impact on solar cell efficiency," in *Proceedings of the 35th IEEE Photovoltaic Specialists Conference*, Honolulu, Hawaii, USA, 2010.

[3] A. Krieg, J. Wallach, and S. Rein, "Impact of surface structures on the inline vision inspection of antireflection coatings," in *Proceedings of the 24th European Photovoltaic Solar Energy Conference*, Hamburg, Germany, 2009, pp. 2041-4.

[4] K. R. McIntosh and S. C. Baker-Finch, "OPAL 2: Rapid optical simulation of silicon solar cells," in *Photovoltaic Specialists Conference (PVSC), 2012 38th IEEE*, 2012, pp. 265-271.

[5] H. A. Macleod, *Thin-film optical filters*: Adam Hilger, 1986.

[6] S. C. Baker-Finch and K. R. McIntosh, "Reflection of normally incident light from silicon solar cells with pyramidal texture," *Progress in Photovoltaics: Research and Applications*, vol. 19, pp. 406-16, 2011.

[7] M. A. Green, "Self-consistent optical parameters of intrinsic silicon at 300 K including temperature coefficients," *Solar Energy Materials & Solar Cells*, vol. 92, pp. 1305-10, 2008.